Research Article | Vol. 7, No. 12 | 1 Dec 2017 | OPTICAL MATERIALS EXPRESS 4408
Optical Materials EXPRESS

Comparison of InGaAs and InAlAs sacrificial layers for release of InP-based devices

J. O'Callaghan,[1] R. Loi,[1,*] E. E. Mura,[1] B. Roycroft,[1] A. J. Trindade,[2] K. Thomas,[1] A. Gocalinska,[1] E. Pelucchi,[1] J. Zhang,[3] G. Roelkens,[3] C. A. Bower,[2] and B. Corbett[1]

[1]*Tyndall National Institute, University College Cork, Lee Maltings, Cork, Ireland*
[2]*X-Celeprint Limited, Lee Maltings, Dyke Parade, Cork, Ireland*
[3]*Ghent University-Imec, Technologiepark-Zwijnaarde 15, Ghent, Belgium*
**ruggero.loi@tyndall.ie*

Abstract: Heterogeneous integration of InP devices to Si substrates by adhesive-less micro transfer printing requires flat surfaces for optimum attachment and thermal sinking. InGaAs and InAlAs sacrificial layers are compared for the selective undercut of InP coupons by $FeCl_3$:H_2O (1:2). InAlAs offers isotropic etches and superior selectivity (> 4,000) to InP when compared with InGaAs. A 500 nm thick InAlAs sacrificial layer allows the release of wide coupons with a surface roughness < 2 nm and a flatness < 20 nm. The InAlAs release technology is applied to the transfer printing of a pre-fabricated InP laser to a Si substrate.

OCIS codes: (130.3130) Integrated optics materials; (130.6622) Subsystem integration and techniques.

References and links

1. E. Menard, K. Lee, Y. Khang, R. Nuzzo, and J. Rogers, "A printable form of silicon for high performance thin film transistors on plastic substrates," Appl. Phys. Lett. **84**, 5398–5400 (2004).
2. M. A. Meitl, Z.-T. Zhu, V. Kumar, K. J. Lee, X. Feng, Y. Y. Huang, I. Adesida, R. G. Nuzzo, and J. A. Rogers, "Transfer Printing by Kinetic Control of Adhesion to an Elastomeric Stamp," Nat. Mater. **5**, 33–38 (2006).
3. A. Carlson, A. M. Bowen, Y. Huang, R. G. Nuzzo, and J. A. Rogers, "Transfer Printing Techniques for Materials Assembly and Micro/Nanodevice Fabrication," Adv. Mater. **24**(39), 5284–5318 (2012).
4. J. Justice, C. Bower, M. Meitl, M. B. Mooney, M. A. Gubbins, and B. Corbett, "Wafer-scale integration of group III-V lasers on silicon using transfer printing of epitaxial layers," Nat. Photonics **6**, 610–614 (2012).
5. J. Yoon, S. M. Lee, D. Kang, M. A. Meitl, C. A. Bower, and J. Rogers, "Heterogeneously Integrated Optoelectronic Devices Enabled by MicroTransfer Printing," Advanced Optical Materials **3**, 1313–1335 (2015).
6. C. Bower, M. Meitl, B. Raymond, E. Radauscher, R. Cok, S. Bonafede, D. Gomez, T. Moore, C. Prevatte, B. Fisher, R. Rotzoll, G. Melnik, A. Fecioru, and A. Trindade, "Emissive displays with transfer-printed assemblies of 8 μm × 15 μm inorganic light-emitting diodes," Photonics Research **5**, A23–A29 (2017).
7. J. Wang, C. Youtsey, R. McCarthy, R. Reddy, N. Allen, L. Guido, J. Xie, E. Beam, and P. Fay, "Thin-film GaN Schottky diodes formed by epitaxial lift-off,", Appl. Phys. Lett. **110**, 173503 (2017).
8. A. J. Trindade, B. Guilhabert, E. Y. Xie, R. Ferreira, J. J. D. McKendry, D. Zhu, N. Laurand, E. Gu, D. J. Wallis, I. M. Watson, C. J. Humphreys, and M. D. Dawson, "Heterogeneous integration of gallium nitride light-emitting diodes on diamond and silica by transfer printing," Opt. Express **23**(7), 9329–9338 (2015).
9. D. Gomez, K. Ghosal, M. A. Meitl, S. Bonafede, C. Prevatte, T. Moore, B. Raymond, D. Kneeburg, A. Fecioru, A. J. Trindade, and C. A. Bower, "Process Capability and Elastomer Stamp Lifetime in Micro Transfer Printing," 2016 IEEE 66th Electronic Components and Technology Conference (ECTC), Las Vegas, (2016).
10. H. Yang, D. Zhao, S. Chuwongin, J. H. Seo, W. Yang, Y. Shuai, J. Berggren, M. Hammar, Z. Ma, and W. Zhou, "Transfer printing stacked nanomembrane lasers on silicon," Nat. Photonics **6**, 617–622 (2012).
11. T. H. Kim, A. Carlson, J. H. Ahn, S. M. Won, S. Wang, Y. Huang, and J. A. Rogers, "Kinetically controlled, adhesiveless transfer printing using microstructured stamps," Appl. Phys. Lett. **94**, 113502 (2009).
12. R. Loi, J. O'Callaghan, B. Roycroft, C. Robert, A. Fecioru, A. J. Trindade, A. Gocalinska, E. Pelucchi, C. A. Bower, and B. Corbett, "Transfer printing of AlGaInAs/InP etched facet lasers to Si substrates," IEEE Photonics J. **8**, 1504810 (2016).
13. A. De Groote, P. Cardile, A. Z. Subramanian, A. M. Fecioru, C. Bower, D. Delbeke, R. Baets, and G. Roelkens, "Transfer-printing-based integration of single-mode waveguide-coupled III-V-on-silicon broadband light emitters," Opt. Express **24**(13), 13754–13762 (2016).
14. X. Sheng, C. Robert, S. Wang, G. Pakeltis, B. Corbett, and J. A. Rogers, "Transfer printing of fully formed thin film micro scale GaAs lasers on silicon with a thermally conductive interface material," Laser Photonics Rev. **9**, L17–L22 (2015).

#308565 https://doi.org/10.1364/OME.7.004408
Journal © 2017 Received 13 Oct 2017; accepted 11 Nov 2017; published 21 Nov 2017

Optical Materials EXPRESS

15. C. W. Cheng, K. T. Shiu, N. Li, S. J. Han, L. Shi, and D. K. Sadana, "Epitaxial lift-off process for gallium arsenide substrate reuse and flexible electronics," Nat. Commun. **4**, 1577 (2013).
16. A. Gocalinska, M. Manganaro, G. Juska, V. Dimastrodonato, K. Thomas, B. A. Joyce, J. Zhang, D. D. Vvedensky, and E. Pelucchi, "Unusual nanostructures of "lattice matched" InP on AlInAs," Appl. Phys. Lett. **104**, 141606 (2014).
17. E. E. Mura, A. Gocalinska, G. Juska, S. T. Moroni, A. Pescaglini, and E. Pelucchi, "Tuning InP self-assembled quantum structures to telecom wavelength: A versatile original InP(As) nanostructure "workshop,"," Appl. Phys. Lett. **110**, 113101 (2017).
18. T. Kusserow, S. Ferwana, T. Nakamura, T. Hayakawa, N. Dharmarasu, B. Vengatesan, and H. Hillmer, "Micromachining of InP/InGaAs multiple membrane/airgap structures for tunable optical devices," Proc. SPIE **6993**, 69930B (2008).

1. Introduction

Micro transfer printing (μTP) is a valuable technique for the heterogeneous integration of photonic, electronic and sensing devices to non-native substrates due to its demonstrated intimate, accurate, parallel and passive alignment capability [1–9]. In the photonics domain μTP has been used to transfer a wide range of LEDs, lasers and photovoltaic cells onto both rigid and flexible target substrates with and without adhesive layers [10, 11]. For applications in telecommunication where the wavelengths of interest range from 1300 nm – 1600 nm it is necessary to use InP-based materials as these provide the most mature structures for lasers, amplifiers, modulators and detectors. The heterogeneous integration of InP-based etched facet lasers onto Si and of LEDs to Si waveguides has been recently demonstrated by using μTP [12, 13]. In order to implement the μTP technique, coupons of material or pre-fabricated devices are prepared, encapsulated and released from their native substrate by the selective etching of an underlying sacrificial layer contained within the layered structure while the devices are held in place using a tethering system. The coupons or devices are attached to the target substrate using an intermediate polymer adhesive layer which can be as thin as 50 nm or by direct van der Waals adhesion if the released surface is flat and smooth enough. The latter adhesive-less situation allows for potential electrical connections and improved heat sinking of the devices. For GaAs devices the release layers have been based on a high Al content AlGaAs layer or AlInP while for the first InP-based devices an InGaAs layer was used [14, 15]. Note that in μTP and in contrast to wafer bonding, the released surface is that used for the attachment and so particular constraints on flatness and smoothness are required.

In this paper, we introduce and characterize InAlAs as an alternative lattice-matched release layer to InGaAs for InP devices. We show that it provides higher selectivity in comparison to InP with much less dependence by the release etchant on the crystal orientation. This enables the orientation of devices along the primary crystal axes and the release of wider coupons without penalty.

2. Experimental

Two epitaxial structures were grown by MOVPE on (100) perfectly oriented InP substrates (+/– 0.1 degree angle) for the purposes of comparing between the different etch release layers. Each release layer (InGaAs, InAlAs) was 500 nm thick, n-doped ($1x10^{18}$ cm^{-3}) with layers of InP adjacent to the release layer. The overgrowth of the InAlAs layer commenced with a thin (10 nm) InGaAs layer to avoid aggregation issues and improve morphology of the InP [16, 17]. Rectangular and circular coupons ranging from 40 μm to 400 μm in width and 50 μm to 500 μm in diameter are realized. The rectangular coupons are orientated at 0, 45, and 90 degrees angle with respect to the major flat of the crystal.

The coupons were fabricated using the sequence shown schematically in Fig. 1. An initial mask of SiO_2 is deposited, patterned and etched to just above the release layer (1). SiN_x is then deposited (2) in order to encapsulate the sidewalls of the coupons, which prevents the coupon material from being etched during the undercut step. The SiN_x is patterned (3) with a slightly wider profile in order to keep the sidewalls of the coupon protected. The encapsulated coupon is wet etched to just above the release layer (4). A SiO_2 passivation layer is deposited

Optical Materials EXPRESS

(5) and patterned as a grating like structure around the coupons. This serves to further encapsulate the coupon and define its base with respect to the release layer. After the SiO_2 layer is etched (6) the structure is etched through the release layer into the substrate to a depth of ~500 nm (7). This exposes the release layer creating a starting point for the coupon release by the undercut etch. Resist anchors 2.8 µm thick are patterned by lithography to restrain the coupon to the substrate during the undercut. The previously defined grating structure prevents resist from entirely covering the sidewalls and blocking exposure of the sacrificial layer. The coupons are undercut (8) and are then available for transfer printing to the target substrate (9).

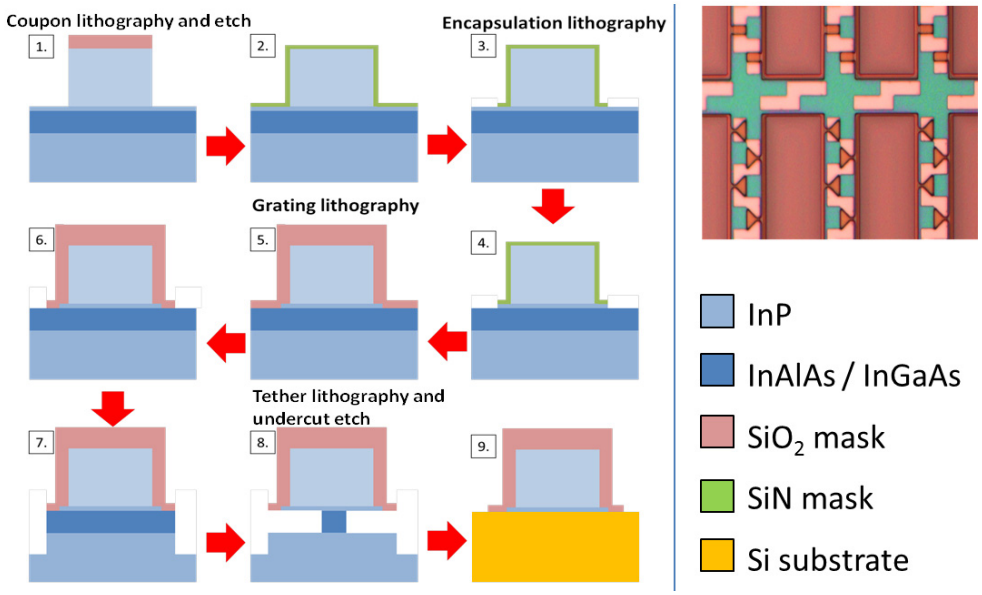

Fig. 1. Schematic of the coupon fabrication process for µTP with steps 1 to 9 as described in the text. The inset (upper right) shows completed tethered coupons prior to µTP. The orange features around the rectangular coupons are the resist tethers while the light green areas between the tethers is the grating structure on the sacrificial layer where the etching starts.

The etching experiments were conducted on both round and rectangular coupons. The selectivity, S, has been calculated as the ratio between the lateral etch rate along the (011) and the $(0\,\bar{1}\,1)$ crystal planes of the sacrificial layer and the vertical etch rate of InP along the <100> crystal axis. $FeCl_3$:H_2O (1:2) iron chloride acid solution was chosen over other etchants for its high selectivity for the target layers over InP [12, 18]. The etch properties were studied for temperatures in the range of 1-20 °C (Fig. 2(a)) as the $FeCl_3$:H_2O (1:2) has been reported to have a maximum selectivity on InGaAs at 6 °C [12]. A cold-tunable plate was used to keep the temperature constant during the etching experiments with an accuracy of ± 0.1 °C.

3. Results and discussion

The InGaAs based coupons were etched for 30, 60, 120, 240 and 360 minutes and the InAlAs coupons were etched for 15, 30, 60 and 120 minutes. Figure 2(b) shows the comparison of the etch depths along the <011> crystal direction as a function of time for the two different sacrificial layers. The etch rate is similar along the $<0\,\bar{1}\,1>$ direction.

The first aspect to note is that the etch rate by the $FeCl_3$:H_2O solution on the InAlAs is over a factor of four higher than that of the InGaAs during the first 60 minutes of etching, when measured along the <011> crystal direction, at 6 °C temperature. The selectivity can be further increased at lower temperatures. It is however desirable to etch at temperatures higher than 1 °C in order to avoid precipitation of the $FeCl_3$ inside the iron chloride solution as this

Optical Materials EXPRESS

could lead to unwanted creation of debris which could affect the print of the devices. The etch rate after 60 minutes starts to decrease gradually due to reduced transport of the etchant under the coupons.

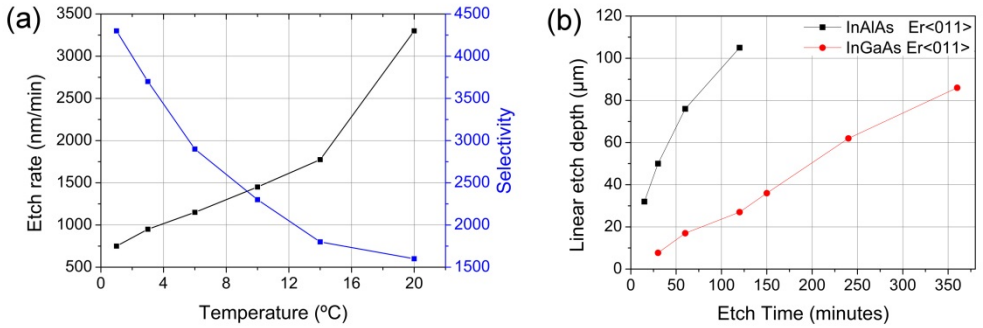

Fig. 2. Etch rate of $FeCl_3$:H_2O (1:2) for the 500 nm thick InAlAs sacrificial layer and its selectivity to InP at different bath temperatures (a). Comparison of etch depths along the <011> crystal directions as a function of time for 500 nm thick InGaAs and InAlAs release layers at 6 °C bath temperature (b).

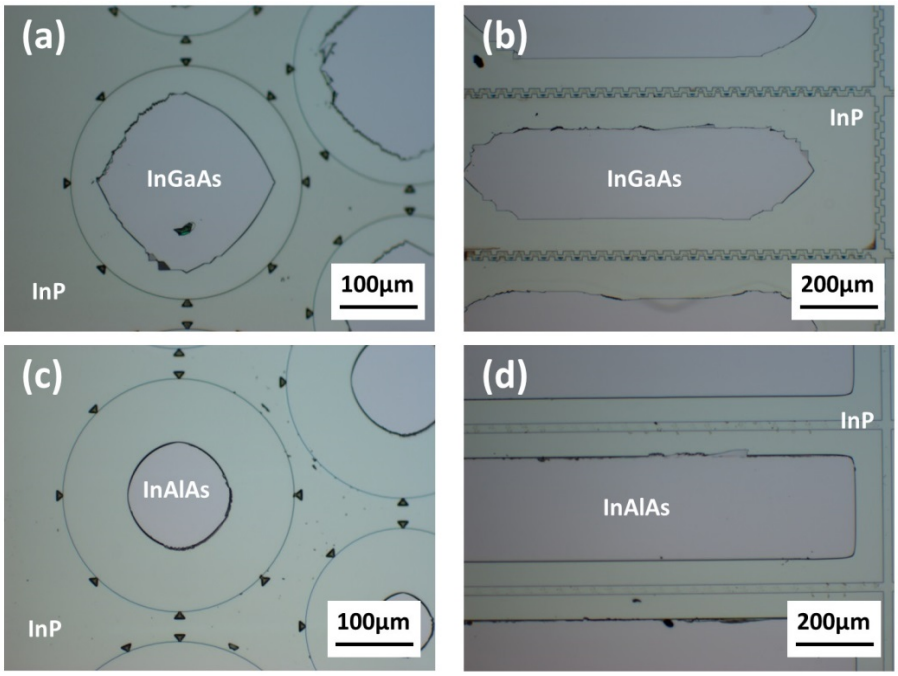

Fig. 3. Comparison of the etch fronts for circular and rectangular coupons containing InGaAs and the InAlAs release layers. The coupons were partially undercut in $FeCl_3$:H_2O (1:2) at 6 °C and peeled off by tape. In this way it is possible to observe the profile of the remaining part of the sacrificial layer. Circular and rectangular coupons with InGaAs release layer after 120 minutes (a) and after 360 minutes (b) etch times show a crystallographic dependent etch front. Similar InAlAs based coupons (c, d) show an isotropic etch profile after 60 minutes.

A second difference between the etched layers is the crystallographic dependence for the evolution of etch front (Fig. 3(a) and 3(b)). The InGaAs based coupons have a high crystallographic dependence on the etch rate with preferential etching along the (001) and the (010) crystal planes whereas the InAlAs based coupons show negligible crystallographic dependence. In the case of the rectangular coupons oriented along the (011) or $(0\,\bar{1}\,1)$ planes

Optical Materials EXPRESS

the InGaAs based coupons show etching from the corners along the (001) and the (010) crystal planes creating a diamond like structure whereas in the InAlAs based coupons show no crystallographic dependency etching evenly around the coupon. Again the undercut etch rates along and at right angles to the (011) plane are over four times higher than those measured in the InGaAs based coupons.

The impact of the higher etch rate and reduced crystallographic dependence on the smoothness and flatness of the coupon surface was further investigated. This was done by examining the coupon site or 'stub' after undercut and removal of the coupon. The coupons are very thin and can be deformed by the presence of the dielectric and resist layers whereas the stub is not. Figure 4 shows the cross section of a stub for a rectangular coupon (110 µm wide and 800 µm long) orientated parallel to the major axis and completely undercut. The cross-sectional profiles were measured across the long axis of the coupon, at the centre, at 200 µm and at 380 µm from the centre of coupon. The InGaAs coupon was undercut for six hours while the InAlAs coupon only required one hour for complete release. A significant difference between the flatness of the coupons is apparent at the centre of the coupon. For the InGaAs based coupons, a height difference of up to 100 nm from the middle of the coupon to the edge is measured. This can be reduced to 30 nm if the coupons are orientated at 45 degrees to the major axis since the undercut time is much reduced. However, this orientation for the coupon may not be suitable for some subsequent processes. Note that this height difference is reduced towards the front of the coupon due to the release layer being undercut earlier at these locations. The height difference from the centre to the edge in the InAlAs coupons is less than 10 nm for a 110 µm wide coupon.

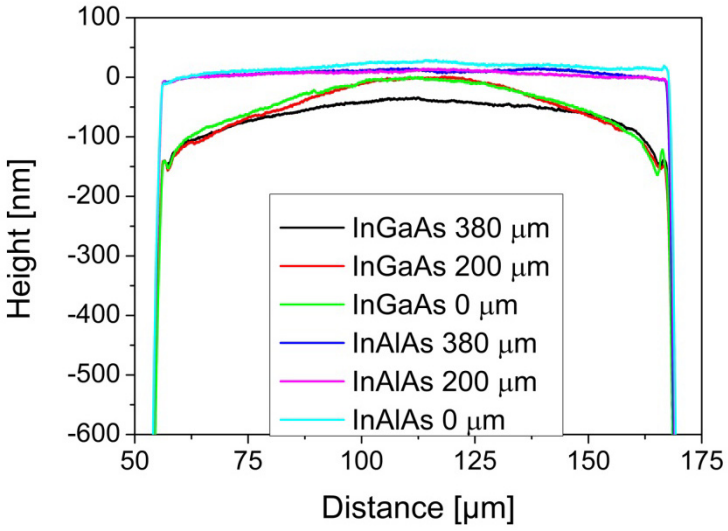

Fig. 4. Plot of the profiles for the stubs from 110 µm wide and 800 µm long coupons including InGaAs and InAlAs release layers. The profiles have been measured at three different positions along the stub, at the centre, at 200 µm and at 380 µm from the centre along the coupon.

The roughness of the stub surfaces, expressed by the Root Mean Square value (RMS), was measured by Atomic Force Microscope (AFM) to be RMS < 9 nm in the case of coupons having InGaAs as the sacrificial layer and etched for 240 minutes. RMS < 2 nm for the InAlAs sacrificial layer. The values of roughness will increase with the etch duration.

To demonstrate the impact of coupon flatness on the transfer print process, we carried out a transfer print on coupons of identical size for each of the release layers. The coupons were picked from their native substrates using a flat piece of polydimethylsiloxane (PDMS). The PDMS is then pressed onto a quartz wafer heated to 90 °C for one minute. The quartz substrate was then viewed from the bottom so as to determine the quality and flatness of the

Optical Materials EXPRESS

print. Figure 5 shows printed coupons from both the InGaAs and InAlAs release layers. Confirming the profilometer plots there is a clear difference in the flatness of coupons for the different release layers.

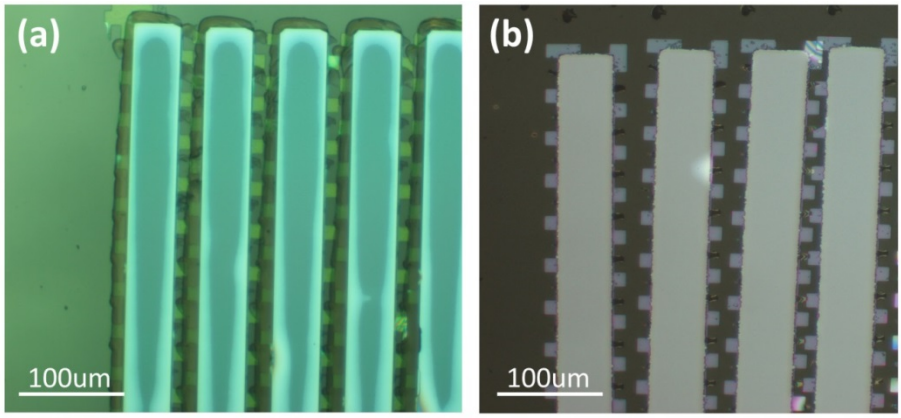

Fig. 5. Microscope images of coupons printed on quartz using an InGaAs (a) and an InAlAs (b) release layer. The InGaAs based coupons show air gaps (lighter colored areas) along the length of the coupon increasing in size towards the centre of the coupon. The InAlAs coupons are monochrome indicating a flat contact with the quartz substrate

If one is relying solely on van der Waals forces for the purposes of bonding, then the flatness and the roughness of the coupons are paramount for good and reliable adhesion. Differences in height can be accommodated by using a thin layer of Benzocyclobutene (BCB) but this excludes the use of direct electrical contact to a substrate and adds an addition step to the μTP process.

Using InAlAs as a release layer is shown to have significant advantages over that of the InGaAs release system in terms of release speed, crystallographic dependence, coupon flatness and roughness. To validate this approach we realized lasers with an InAlAs release layer and fabricated etched facet ridge waveguide lasers with high reflective coating at one of the facets. Figure 6 shows the light current characteristics and the lasing spectrum from such devices. The light current (LI) characteristics are approximated by collecting part of the emitted light with a 3 mm diameter Ge detector placed at a few mm from the lasers on the original substrate and on the Si substrate. The lasers were injected in continuous wave mode. The lasers before and after transfer have similar threshold current, at about 19 mA at 20 °C (Fig. 6 (a)). The emission spectrum was collected by using a multimode fiber positioned at a few millimeters in front of the emitting facet of a laser printed on Si (Fig. 6(b)). The main emission peak is at about 1554 nm wavelength at room temperature. The free spectral range of the resonator is at $\Delta\lambda = 0.66$ nm as expected for a 500 μm long Fabry-Perot resonant cavity. This experiment demonstrates that the InAlAs layer offers a suitable approach for the release of transfer printable InP based devices.

Optical Materials EXPRESS

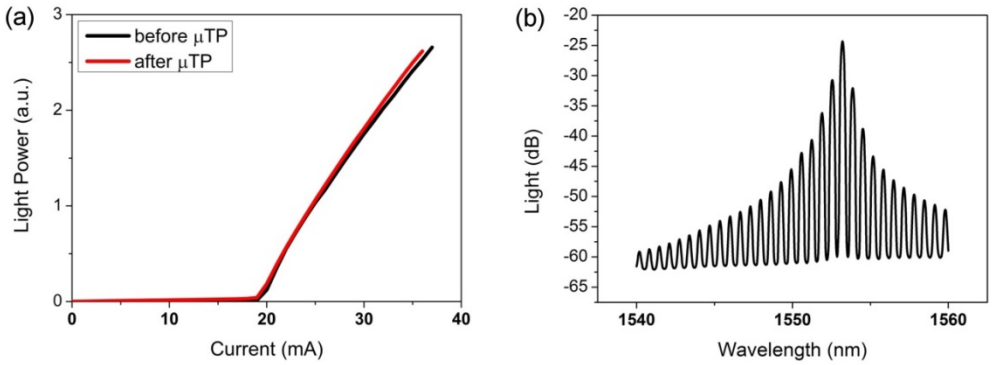

Fig. 6. Light current characteristics at 20 °C for a laser using the InAlAs layer in its release structure, before and after μTP to a Si substrate (a). Lasing spectrum from a printed device (b).

4. Conclusions

A novel InAlAs/InP release structure for the release of InP based optical devices has been introduced. The etch rate of the InAlAs was compared to that of the InGaAs using iron chloride. The InAlAs proved to be superior to InGaAs in terms of etch rate and reduced crystallographic dependence that allows coupons to be freely orientated. The higher etch rate of InAlAs allows the release of coupons of 100 μm width in < 50 minutes while keeping a deviation from the flatness < 5 nm over a 100 μm length. In comparison an InGaAs release structure oriented along the (011) crystal plane results in surfaces with a significant height profile making transfer printing more difficult without using an adhesive layer. A ridge waveguide laser based on the InAlAs release layer was fabricated further showing the viability of the release layer when applied to photonic structures. This approach forms the basis for the adhesive-less integration of large area InP based devices to Si substrates while providing high quality surfaces suitable for high quality thermal and electrical contacts. It can also be applied in many other technological situations such as in the formation of air-bridges for high speed interconnects.

Funding

Science Foundation Ireland (12/RC/2276 (IPIC) and 15/IA/2864); European Union's Horizon 2020 Research and Innovation Programme (45314 (TOP-HIT)).